sidered in the regression analysis. The most impressive feature of this prediction is its applicability over a weight variation of six orders of magnitude.

It should be reiterated that this correlation is for conventional aircraft designs of moderate to high aspect ratio in the cruise configuration. As such, this equation predicts the noise "floor" for aircraft with today's technology. That is, it represents the minimum power-off noise that can be achieved by simple aerodynamic cleanup.

These empirical predictions of OASPL directly beneath an aircraft during flyover give no information about the frequency content of the observed noise. However, Healy[5] used smoothed spectra from clean configured aircraft to define the nondimensional noise spectrum illustrated in Fig. 3. He suggests that the frequency at which the spectrum peaks can be determined from a Strouhal relation, leading to the equation

$$f_{\max} = 1.30(V/t) \tag{3}$$

where V is velocity, and t is a representative wing thickness taken at the wing station whose chord is equal to wing area divided by wing span. The dashed curves in Fig. 4 are the boundaries within which his measured data fell. More recently, Ref. 6 has presented some data on a very large aircraft (C5-A) wherein the spectrum peak was found to be narrower although the frequency at which the peak occurred agreed reasonably well with this prediction.

Landing Configurations

The approaches just discussed assumed that airframe noise would be very configuration dependent for aircraft on landing approach due to flaps and landing gear exposed to the airstream. Therefore, to account for "dirty" configuration noise generation, both Healy and Hardin suggest that the OASPL predicted for clean airframes be increased by 5-6 db. This factor was found by both investigators to predict the landing configuration noise within the accuracy expected for preliminary design purposes, and required no additional information about the aircraft under study.

Recently, Revell[9] has proposed an alternate predictive scheme that directly predicts airframe noise of any configuration if its drag parameters are known. He bases his semiempirical theory on the assumption that airframe noise is a byproduct of mechanical energy dissipated by drag. He then uses the spectral sum of three assumed major sources of dipole noise: 1) wing profile drag, 2) wing induced drag, and 3) fuselage and landing gear drag, to arrive at a predictive equation of the form:

$$\text{OASPL} = 10 \log_{10}[C_D^2 V^6 S/r^2] + K_3 \tag{4}$$

Both similarities and differences to Eqs. (1) and (2b) are apparent. For instance, for a clean lifting wing where induced drag produces the dominant noise and $C_{Di} \sim 1/A$, this procedure would predict the same dependence on aspect ratio as Eq. (2b). The spectrum employed in this approach is more complicated than the generalized spectrum used by the earlier methods (Fig. 3) since each of the three drag components contributes. Although this method has only been applied to a limited number of cases, it promises to be very useful since readily available drag data are sufficient for its application.

Results

The ability of these methods to predict the approach noise of commercial-type aircraft at the FAR Part 36 measuring point is illustrated in Fig. 4. Approach noise, in EPNdb, is shown as a function of gross take-off weight for several aircraft. The open symbols represent the certificated noise levels for the latest generation aircraft and are all below the FAR Part 36 standard. This measured noise consists of the summation of noise from all sources on the aircraft, but engine noise dominates. The method of Hardin, Eq. (2b), was used to predict the clean airframe noise, indicated by the closed symbols. Effective perceived noise level values were estimated assuming a level flyover at approach velocity, dipole directivity, and the predicted OASPL level and the nondimensional spectrum given in Fig. 3. These values are seen to be about 15 EPNdb, on the average, below the certificated noise levels. Since the aircraft are in the approach configuration, 5-6 EPNdb must be added to the calculations to account for noise generated by "dirty" aerodynamics associated with flaps and landing gear. This brings the total airframe noise for these aircraft to the level indicated by the dashed area, approximately 10 EPNdb below the FAR Part 36 standard. The prediction method of Revell, Eq. (4), is also reported in Ref. 9 to predict an airframe noise level about 10 EPNdb below those specified in FAR Part 36. The credibility of these predictions is enhanced in Ref. 2 which reported engine-idle flight tests with B-727 aircraft that established their approach airframe noise levels at the certification measuring point as about 8 EPNdb below the FAR Part 36 standard.

Figure 4 shows that engine noise must be reduced another 5-8 EPNdb in the current generation aircraft before airframe noise becomes a significant factor in certification measurements. But it also shows that, if engine noise could be reduced still further, about 5-6 EPNdb of airframe noise reduction could be achieved by working on aerodynamic cleanup before hitting the clean airframe floor. Thus, the first payoffs in airframe noise reduction can be up to about 5 EPNdb by reducing the noise generated by flows around flaps, landing gear, and cavities.

References

[1]Gibson, J. S., "The Ultimate Noise Barrier-Far Field Radiated Aerodynamic Noise," *Proceedings of the International Conference on Noise Control Engineering,* INCE and ASA, Washington, D. C., Oct. 4-6, 1972, pp. 332-337.

[2]Blumenthal, V. L., Streckenbach, J. M., and Tate, R. B., "Aircraft Environmental Problems," AIAA Paper 73-5, Jan. 1973, Washington, D. C.

[3]Hayden, R. E., "Fundamental Aspects of Noise Reduction From Powered Lift Devices," SAE Preprint 730376, April 1973, Society of Automotive Engineers, New York, N.Y.

[4]Gibson, J. S., "Recent Developments at the Ultimate Noise Barrier," *9th Congress of the International Council of the Aeronautical Sciences,* Haifa, Israel, Paper 74-59, 1974.

[5]Healy, G. J., "Measurement and Analysis of Aircraft Far-Field Aerodynamic Noise," CR-2377, 1974, NASA.

[6]Gibson, J. S., "Non-Engine Aerodynamic Noise Investigation of a Large Aircraft," CR-2378, 1973, NASA.

[7]Burley, R. R., "Preliminary Measurement of the Airframe Noise From an F-106B Delta Wing Aircraft at Low Flyover Speeds," TM X-71527, March 1974, NASA.

[8]Hardin, J. C., Fratello, D. J., Hayden, R. E., Kadman, Y., and Africk, S., "Prediction of Airframe Noise," TN D-7821, 1975, NASA.

[9]Revell, J. D., "Calculation of Aerodynamic Noise Generated by Large Aircraft at Landing Approach," *presented at the 87th Meeting of the Acoustical Society of America,* New York, 1974.

Propulsive Effects due to Flight through Turbulence

William H. Phillips*
NASA Langley Research Center, Hampton, Va.

Introduction

THE production of thrust on an airfoil subject to an oscillating airflow has been called the "Katzmayr Effect."[1] Flight through random turbulence would be expected to produce a similar propulsive effect,

Received January 3, 1975; revision received February 24, 1975.
Index categories: Aircraft Gust Loading and Wind Shear; Aircraft Performance.

*Chief, Flight Dynamics and Control Division. Fellow AIAA.

although lack of any noticeable performance gains on actual airplanes in flight through turbulence indicates the effect is probably quite small. There has been some speculation that modern, highly-efficient soaring gliders might be able to derive a performance gain from flight through turbulence. This report presents a simplified analysis which indicates the approximate magnitude of the propulsive effect for various types of airplanes. The performance gain at very low frequencies from so-called "dolphin soaring," in which a glider is flown slowly in regions of updrafts and fast in regions of downdrafts, is not considered because the airspeed is assumed constant.

Analysis

A brief physical explanation of the major propulsive effects of flight through turbulence may be obtained from consideration of changes in the magnitude and direction of the lift vector. An upward gust increases the lift and tilts the lift vector forward. A downward gust decreases the lift and tilts the lift vector rearward. The net result is an increased average forward component of force acting on the wing. Changes in the drag component tend to reduce this thrust, but for efficient wings, the effects of tilting the lift vector predominate. As the airplane penetrates an upward gust, it responds by rising, quickly acquiring the vertical velocity of the surrounding air mass. This motion of the airplane decreases the duration of the changes in lift, thereby reducing the average propulsive effect. The combined effect of the gust velocity variations and the airplane response must, therefore, be considered in calculating the average propulsive effect. Any possible change in thrust from the aircraft propulsion system due to flight through turbulence is neglected in this analysis.

The airplane, subject to vertical gust disturbances, is assumed to be constrained to fly at constant airspeed and constant pitch angle. This assumption is a good approximation to the behavior of an airplane under the control of a human pilot or an autopilot. The lift and drag coefficients, C_L and C_D, are represented as linear and quadratic functions, respectively, of the angle of attack, α. If the components of lift and drag along the flight path are summed, and the terms sin α and cos α are expanded in Taylor series, the expression for the change in coefficient of thrust is, to the second order in α:

$$C_T = \alpha(C_{L_I} - C_{D_\alpha}) + \alpha^2(C_{L_\alpha} - C_{D_{\alpha^2}} + C_{D_I}/2) \qquad (1)$$

where C_{L_I} and C_{D_I} are the trim values of C_L and C_D. The small term $C_{D_I}/2$, which amounts to only about 1% of C_{L_α}, is omitted in subsequent calculations because it may be shown to be approximately offset by the slightly increased drag due to horizontal gust fluctuations.

The value of α is the total angle of attack resulting from the gust input α_g and the vertical motion of the airplane. Inasmuch as the vertical response of the airplane is represented as a linear system, and α_g is assumed to be a Gaussian random process with zero mean, the terms multiplied by the first power of α will likewise have zero mean and will not contribute to the average thrust.

The terms multiplied by α^2 have an effect similar to passing a random signal through a square law device, a process considered in Ref. 2. The formula for the mean value of the output states that the mean value of the thrust, $\bar{C}_T$, is simply the product of the constant K and the variance, or mean-square value, of α. Hence:

$$\bar{C}_T = K\sigma_\alpha^2 \qquad \text{where} \qquad K = C_{L_\alpha} - C_{d_{\alpha^2}} \qquad (2)$$

The variance of α may be obtained as the area under the power spectrum of α, which is the power spectrum of the gust input, $\Phi_{\alpha_g}(\omega)$, multiplied by the square of the transfer function relating α to α_g. Hence

$$\bar{C}_T = K\int_0^\infty \Phi_{\alpha_g}(\omega)\ |\alpha/\alpha_g|^2 d\omega \qquad (3)$$

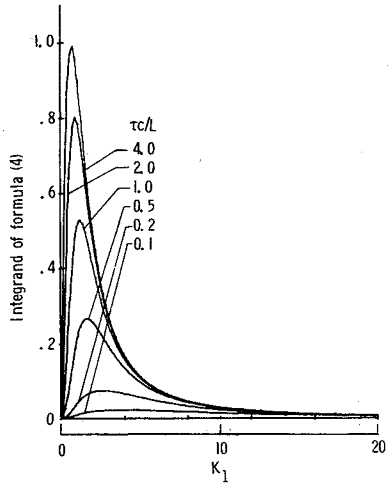

Fig. 1 Variations of contributions to mean thrust with nondimensional frequency K_1.

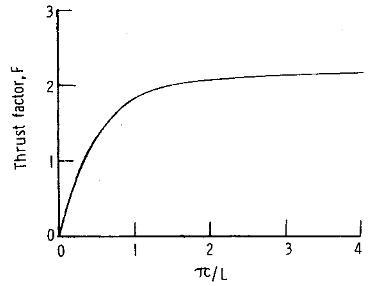

Fig. 2 Variation of thrust factor F with $\tau c/L$.

$$\bar{C}_T = (K\bar{w}_g{}^2 F)/(\pi V^2)$$

Table 1 Characteristics of airplanes[a]

Type	mass, kg	S, m^2	c, meters	C_{L_α}, per rad	$C_{D_{\alpha^2}}$, per rad^2
Soaring glider	408	13.0	0.7	5.8	0.45
Light airplane	1,000	16.0	1.5	4.9	1.09
Fighter	18,000	25.0	2.5	4.5	1.29
Transport	35,000	85.0	3.5	5.1	1.03

[a] S = wing area, c = wing chord.

The integrand of Eq. (3) does not represent the power spectrum of the thrust coefficient, because the oscillatory components of the response are ignored. This curve, instead, represents the contribution in each increment of frequency to the mean thrust.

The assumptions made for the atmospheric gust spectrum and for the airplane response are as follows. For the gust spectrum, the Dryden spectrum is assumed:

$$\frac{\Phi_{w_g}\pi V}{L\bar{w}_g{}^2} = \frac{1+3K_1{}^2}{(1+K_1{}^2)^2}$$

where $K_1 = \omega L/V$. In these formulas, Φ_{w_g} is the power spectrum of vertical gust velocity, L is the scale of turbulence, V is the airspeed, and ω is the frequency in rad/sec. For the airplane, assumed free to move vertically but constrained in speed and pitch angle, $\alpha_o/\alpha_g = -(\tau' D + 1)^{-1}$ where $D = d(\ )/dt$ and $\tau' = \tau c/V$, where $\tau = 2\mu/C_{L_\alpha}$ and μ, the relative density factor, is $m/\rho Sc$, where m = mass, S = wing area, and c = wing chord. Hence $\alpha/\alpha_g = \alpha_o/\alpha_g + 1 = \tau' D/(\tau' D + 1)$. Substituting $D = i\omega$, the real and imaginary parts of the response may be obtained in the form

Table 2 Response time and thrust coefficient due to turbulence[a]

Type	V, m/sec	τ, chords	$\tau c/L$	$\bar{C}_T$, $\bar{w}_g = 1$m/sec	$\bar{C}_T$, 2m/sec	$\bar{C}_T$, 4m/sec
Soaring glider	22.0	12.0	0.028	0.00032	0.0013	0.0050
Light airplane	30.9	13.2	0.066	0.00030	0.0012	0.0049
Fighter	105.0	99.5	0.829	0.00016	0.00063	0.0025
Transport	64.7	35.8	0.417	0.00024	0.00098	0.0039

[a] $L = 300$ m, $C_L = 1.0$ (sea level).

$\alpha/\alpha_g = A(\tau'\omega) + iB(\tau'\omega)$. Substituting these values in Eq. (3) for the mean thrust coefficient gives:

$$\bar{C}_T = \frac{K\bar{w}_g^2}{\pi V^2} \int_0^\infty \frac{1+3K_l^2}{(1+K_l^2)^2} (A^2+B^2)\mathrm{d}K_l \qquad (4)$$

where A and B must be expressed in terms of the nondimensional frequency K_l. Since A and B are functions of $\tau'\omega$, and $\tau'\omega = (\tau c/V)(K_l V/L) = (\tau c/L)K_l$, the quantity under the integral sign is a function of the parameter $\tau c/L$. Physically, this quantity represents the ratio of the distance for subsidence of the airplane motion to the scale of turbulence.

Results and Discussion

A plot of the integrand of Eq. (4) as a function of K_1 for various values of the parameter $\tau c/L$ is shown in Fig. 1. The value of the integral, labeled thrust factor, F, as a function of $\tau c/L$ is shown in Fig. 2. As shown in Fig. 1, for all except very small values of $\tau c/L$, most of the thrust comes from low frequency components of turbulence, and the area under the curve is not much affected by the upper frequency limit assumed. For very small values of $\tau c/L$ (less than 0.02) however, the contributions to the thrust are nearly uniform throughout the frequency range. The effect of unsteady lift and spanwise gust variations, which attenuate the lift variations at high frequencies, was approximated by taking the upper frequency limit of the integration as $K_l = 20\pi$.

To show the significance of the results given in Fig. 2, calculations have been made for several typical airplane types having the characteristics given in Table 1. The estimated values of thrust coefficient due to flight through turbulence having scale length L of 300 m and root-mean-square gust velocities of 1, 2, and 4 m/sec are shown in Table 2. These values are shown for a lift coefficient of 1.0 at sea level. The values of thrust coefficient vary directly with lift coefficient because of the effect of lift coefficient on airspeed and hence on the term $\bar{w}_g^2/V^2$. The thrust coefficient, therefore, decreases at higher flight speeds. The thrust coefficient has been found to be little affected by increasing altitude for the soaring glider and the light airplane, but to decrease with increasing altitude for the fighter and transport.

In the case of lightly loaded airplanes flying at low airspeed, the angle-of-attack variation due to gusts, $\bar{w}_g/V$, is relatively large, but the short response time constant of these airplanes allows them rapidly to assume the vertical velocity of the surrounding air mass, thereby reducing the thrust contributions of low-frequency gusts which contain most of the energy of turbulence. More heavily loaded airplanes, on the other hand, produce less attenuation of the effects of the low-frequency gusts, but because of their higher airspeed, the value of $\bar{w}_g/V$ in turbulence of a given intensity is reduced. As shown by Table 2, the resulting effect is to give about the same relatively low value of thrust coefficient for each of the airplane types in flight at given values of lift coefficient and turbulence intensity.

In conclusion, the thrust effects due to turbulence vary as the square of the turbulence intensity and are quite small for moderate turbulence. Only for rather severe turbulence are the effects large enough to be given any consideration. In the case of a soaring glider in turbulence with a root-mean-square velocity of 4 m/sec, the thrust coefficient due to the turbulence at $C_L = 1.0$ is about 0.005. For typical soaring gliders, the value of L/D at $C_L = 1.0$ might range from 20 to 40. The thrust coefficient is therefore from 10 to 20% of the drag coefficient of the glider. In view of the large disturbances of the flight path in turbulence of this magnitude, it is doubtful that the effect would be noticeable.

References

[1] Katzmayr, R., "Effect of Periodic Changes of Angle of Attack on Behavior of Airfoils," TM147, Oct. 1922, NACA.

[2] Davenport, W. B., Jr. and Root, W. L., *An Introduction to the Theory of Random Signals and Noise,* McGraw-Hill, New York, 1958, Chap. 12, formula (12-23), p. 225.

Prediction of Span Loading from Measured Wake-Vortex Structure —An Inverse Betz Method

Vernon J. Rossow*
NASA Ames Research Center, Moffett Field, Calif.

Introduction

A THEORETICAL tool frequently used to study the circumferential velocity distribution in lift-generated vortices is the simple rollup method of Betz.[1] His theory is based on the conservation equations for inviscid, two-dimensional vortices and predicts the circulation in the fully-developed vortex from the span loading on the generating wing. This relationship between span loading and vortex structure is extended here by introducing a so-called inverse rollup method that predicts the span loading on the generating wing when the radial distribution of circumferential velocity in the vortex is given. After the equations to be used in the theory are derived, several examples are presented wherein measured circumferential velocities in several vortices are used with the inverse method to infer the span loading that produced the vortices. These span loadings are compared with those predicted by vortex-lattice theory for the generating wing.

Derivation of Inverse Rollup Method

As mentioned in the Introduction, the existing or direct Betz method[1] for the structure of fully-developed vortices is based on the conservation laws for two-dimensional vortices; i.e., conservation of circulation and of the first and second moments of circulation. To achieve a unique result, the vortex sheet is assumed to roll up in an orderly fashion from the wing tip inboard so that successive layers of the sheet are wrapped around the center and over previous wrappings (Fig. 1 of Ref. 2). Any axial or streamwise variation in the flow velocity is

Received November 4, 1974; revision received January 24, 1975.
Index categories: Aircraft Aerodynamics (including Component Aerodynamics); Jets, Wakes, and Viscid-Inviscid Flow Interactions; Aircraft Flight Operations.

*Staff Scientist. Associate Fellow AIAA.